Structural Analysis of *Pseudomonas* 1-Aminocyclopropane-1-carboxylate Deaminase Complexes: Insight into the Mechanism of a Unique Pyridoxal-5′-phosphate Dependent Cyclopropane Ring-Opening Reaction[†,‡]

Subramanian Karthikeyan,[§] Qingxian Zhou,[§] Zongbao Zhao,[||] Chai-Lin Kao,[||] Zhihua Tao,[||] Howard Robinson,[⊥] Hung-wen Liu,*[,||] and Hong Zhang*[,§]

Department of Biochemistry, University of Texas Southwestern Medical Center, Dallas, Texas 75390-9038, Division of Medicinal Chemistry, College of Pharmacy, and Department of Chemistry and Biochemistry, University of Texas, Austin, Texas 78712, and National Synchrotron Light Source, Brookhaven National Laboratory, Upton, New York 11973

Received June 1, 2004; Revised Manuscript Received August 12, 2004

ABSTRACT: 1-Aminocyclopropane-1-carboxylate (ACC) deaminase is a pyridoxal 5′-phosphate (PLP) dependent enzyme catalyzing the opening of the cyclopropane ring of ACC to give α-ketobutyric acid and ammonia as the products. This ring cleavage reaction is unusual because the substrate, ACC, contains no abstractable α-proton and the carboxyl group is retained in the product. How the reaction is initiated to generate an α-carbanionic intermediate, which is the common entry for most PLP-dependent reactions, is not obvious. To gain insight into this unusual ring-opening reaction, we have solved the crystal structures of ACC deaminase from *Pseudomonas* sp. ACP in complex with substrate ACC, an inhibitor, 1-aminocyclopropane-1-phosphonate (ACP), the product α-ketobutyrate, and two D-amino acids. Several notable observations of these structural studies include the following: (1) a typically elusive *gem*-diamine intermediate is trapped in the enzyme complex with ACC or ACP; (2) Tyr294 is in close proximity (3.0 Å) to the *pro-S* methylene carbon of ACC in the *gem*-diamine complexes, implicating a direct role of this residue in the ring-opening reaction; (3) Tyr294 may also be responsible for the abstraction of the α-proton from D-amino acids, a prelude to the subsequent deamination reaction; (4) the steric hindrance precludes accessibility of active site functional groups to the L-amino acid substrates and may account for the stereospecificity of this enzyme toward D-amino acids. These structural data provide evidence favoring a mechanism in which the ring cleavage is induced by a nucleophilic attack at the *pro-S* β-methylene carbon of ACC, with Tyr294 as the nucleophile. However, these observations are also consistent with an alternative mechanistic possibility in which the ring opening is acid-catalyzed and may be facilitated by charge relay through PLP, where Tyr294 functions as a general acid. The results of mutagenesis studies corroborated the assigned critical role for Tyr294 in the catalysis.

1-Aminocyclopropane-1-carboxylate (ACC,[1] **1**, Scheme 1) is the precursor for the biosynthesis of ethylene, a plant hormone that regulates fruit ripening and other aspects of plant growth and development (*1*, *2*). In higher plants, ACC is formed from *S*-adenosylmethionine (SAM) via a ring-closing γ-displacement reaction catalyzed by ACC synthase (*3*, *4*). ACC is then oxidized by ACC oxidase to form ethylene (*2*, *5*). In several bacteria and yeast species, ACC can also be converted to α-ketobutyrate (α-KB, **2**) and ammonia by ACC deaminase (*6*, *7*). It has been shown that introduction of bacterial ACC deaminase into higher plants by gene technology reduces the production of ethylene, delays the ripening progression of fruits, and extends the shelf life of fruits and vegetables (*8*, *9*).

ACC deaminase is a pyridoxal 5′-phosphate (PLP) dependent enzyme catalyzing an unusual cyclopropane ring-opening reaction. For most PLP-dependent enzymes, the reaction starts with the conversion of an internal aldimine between PLP and an active site lysine residue (such as **3**) to an external aldimine between PLP and the amino group of the substrate (such as **5**). The next step is the removal of the α-proton of the substrate, which triggers subsequent trans-

[†] This work was supported in part by grants from the National Institutes of Health (GM63689 to H.Z. and GM40541 to H.-w.L.).

[‡] The atomic coordinates and the structure factors for *Pseudomonas* ACC deaminase complexes have been deposited in the Protein Data Bank (PDB; http://www.rcsb.org/pdb/). The accession codes are 1tyz (native enzyme), 1tz2 (complex with ACC), 1tzm (complex with β-Cl-D-Ala), 1tzj (complex with D-vinylglycine), and 1tzk (complex with α-ketobutyric acid).

* To whom correspondence should be addressed. Tel: 214-648-9299 (H.Z.) and 512-232-7811 (H.-w.L.). Fax: 214-648-9099 (H.Z.) and 512-471-2746 (H.-w.L.). E-mail: zhang@chop.swmed.edu (H.Z.) and h.w.liu@mail.utexas.edu (H.-w.L.).

[§] University of Texas Southwestern Medical Center.

[||] University of Texas.

[⊥] Brookhaven National Laboratory.

[1] Abbreviations: ACC, 1-aminocyclopropane-1-carboxylic acid; ACP, 1-aminocyclopropane phosphonate; β-Cl-D-Ala, β-chloro-D-alanine ((2*S*)-3-chloroalanine); DMAPP, dimethylallyl diphosphate; HOMO, highest occupied molecular orbital; IPP, isopentenyl diphosphate; α-KB, α-ketobutyric acid; MACC, 1-amino-2-methylenecyclopropane-1-carboxylic acid; NADH, β-nicotinamide adenine dinucleotide, reduced form; PCR, polymerase chain reaction; PEG, poly(ethylene glycol); PLP, pyridoxal 5′-phosphate; SAM, *S*-adenosylmethionine; SDS, sodium dodecyl sulfate; TMS, tetramethylsilane; D-VG, D-vinylglycine ((2*R*)-vinylglycine); rmsd, root-mean-square deviation.

10.1021/bi048878g CCC: $27.50
Published on Web 09/29/2004

Scheme 1

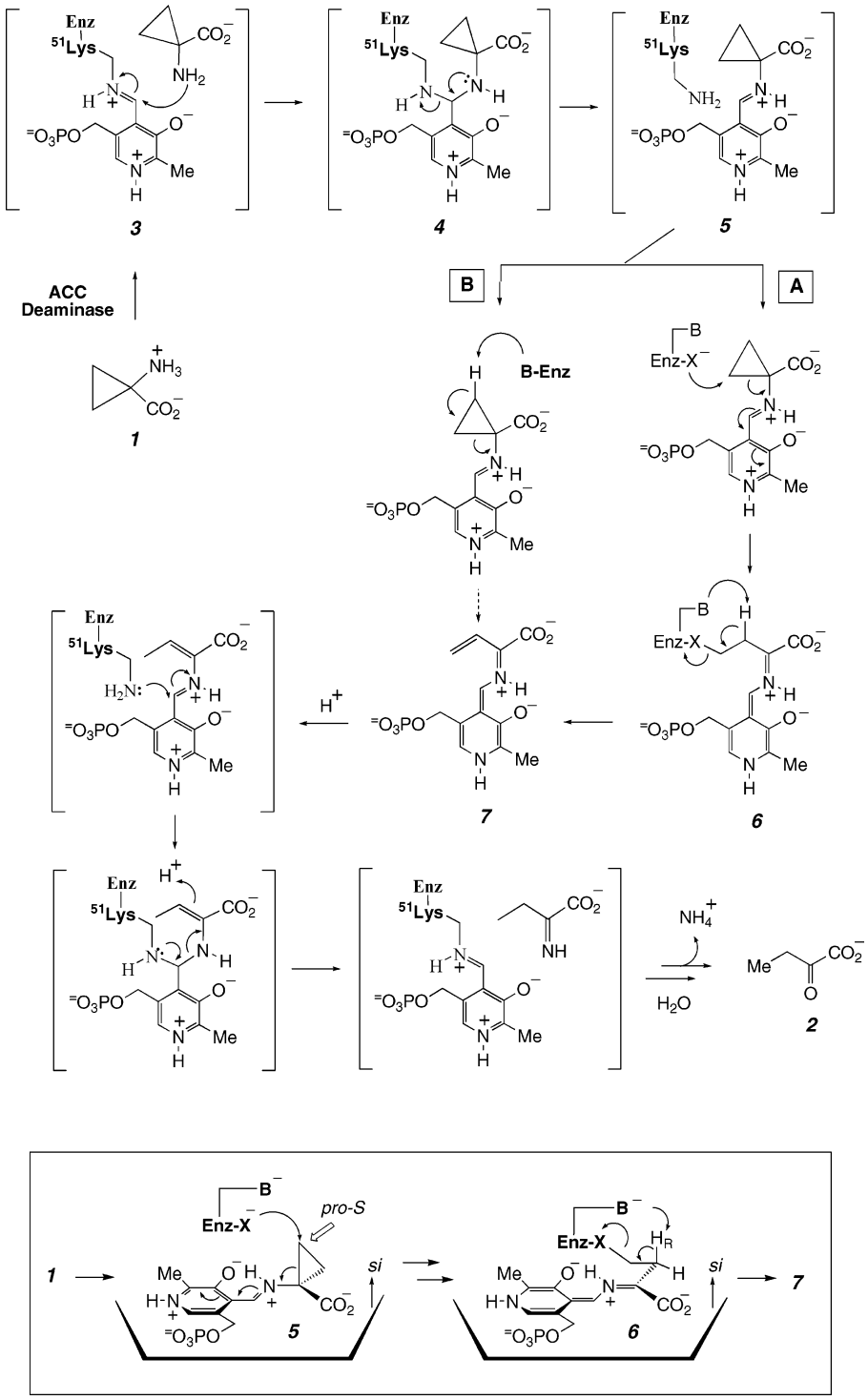

formations such as transamination, racemization, β- and γ-elimination, and replacement reactions (*10*, *11*). In contrast, for the PLP-dependent decarboxylation of an α-amino acid, it is the elimination of the α-carboxyl group that initiates the reaction. Interestingly, ACC (**1**) has no abstractable α-hydrogen and its carboxyl group is retained in the product. Hence, the cyclopropane ring opening of ACC catalyzed by ACC deaminase must be initiated without obvious accessibility to an α-carbanionic intermediate.

Substantial studies of this unusual enzyme have been conducted over the past several years aimed at unraveling the mechanism of this unprecedented ring-opening reaction (*7*, *12*−*17*). The α-anion equivalent of vinylglycyl-PLP aldimine (**7**) has been suggested to be a key reaction intermediate, which led to the proposal of two possible routes for the ring fragmentation: (1) nucleophilic addition at the C_β methylene position to open the ring followed by β-proton abstraction (Scheme 1, route A); (2) β-proton abstraction leading directly to the cleavage of the cyclopropane ring (Scheme 1, route B) (*12*). The stereospecificity of the reaction has also been determined in which the cyclopropane ring is cleaved specifically between C_α and *pro-S* C_β of the ring (Scheme 1) (*13*, *14*). Thus far, the majority of the data favors the nucleophilic addition initiated route (route A). The direct

β-proton abstraction route is considered unlikely because it requires the abstraction of a nonacidic proton from the cyclopropane methylene group. One compelling piece of evidence supporting the nucleophilic addition mechanism is the observation that the ACC analogue, 2-methylene-ACC (MACC, **8**), which has a more strained cyclopropane ring, is a better substrate than ACC (*16*, *17*). This result is most consistent with the nucleophilic addition mechanism for the ring cleavage. However, the full understanding of the exact mode of cyclopropane ring scission by ACC deaminase requires the elucidation of the three-dimensional conformation of the enzyme active site and the detailed interactions between functional groups of the enzyme and the substrate.

Herein, we report high-resolution crystal structures for ACC deaminase from *Pseudomonas* sp. strain ACP in its native form and in complexes with the substrate ACC (**1**), the product α-ketobutyrate (**2**), an inhibitor, 1-aminocyclopropane phosphonate (ACP, **9**), and D-vinylglycine (D-VG, **10**) and β-chloro-D-alanine (β−Cl-D-Ala, **11**), which serve as alternative substrates. One notable highlight of these

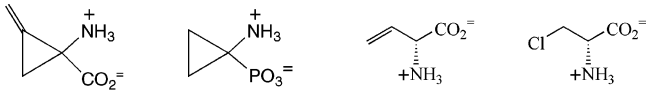

8 **9** **10** **11**

structural studies is the revelation of a *gem*-diamine (an aminyl) adduct between the PLP cofactor and the substrate/inhibitor, such as **4**, in the enzyme−substrate/inhibitor complexes, representing a rare example of a transient intermediate that is trapped during turnover. The crystal structure also reveals that Tyr294 is proximal to the *pro-S* methylene of the cyclopropane ring and likely plays a critical role in catalysis. These data provide the structural basis supporting route A as the favored mechanism for ring cleavage catalyzed by ACC deaminase with Tyr294 as the nucleophile. However, these observations are also consistent with an alternative mechanism in which ring opening is an acid-catalyzed event where Tyr294 functions as the putative general acid. A preliminary analysis of the enzyme−ACP (**9**) complex had been reported (*18*). A full account of the structural studies of the above series of enzyme substrate/inhibitor complexes and the mechanistic implications of these data are detailed herein.

MATERIALS AND METHODS

General. NMR spectra were recorded on a Varian 500 MHz spectrometer. Chemical shifts (δ in ppm) are given relative to those for TMS (for ^{1}H and ^{13}C), with coupling constants in hertz (Hz). The concentration of protein was determined by the Bradford method (*19*) using bovine serum albumin as the standard. The purity of enzyme samples was determined using SDS−polyacrylamide gel electrophoresis. DNA sequencing was conducted by the ICMB Core Labs of the University of Texas at Austin. Plasmid pQNt23, used as the PCR (polymerase chain reaction) template for the ACC deaminase gene, was prepared in a previous study (*16*). The pET-17b(+) vector and overexpression host strain *Escherichia coli* BL21(DE3)/pLysS were purchased from Novagen Inc. (Madison, WI). Culture media were products of Difco (Detroit, MI). All electrophoretic reagents, except for the DNA ladders (100 bp and 1 kp) and agarose, which were obtained from Gibco BRL (Grand Island, NY), were products of Bio-Rad (Hercules, CA). Oligonucleotides used in PCR amplification of desired inserts were prepared by Gibco BRL and used without further purification. Restriction endonucleases were either from Gibco BRL or Promega (Madison, WI). α-Ketobutyric acid (**2**) and β-chloro-D-alanine (**11**) were purchased from Sigma-Aldrich (St. Louis, MO)

Crystallization and Data Collection. The cloning, expression, and purification of the wild-type *Pseudomonas* ACC deaminase had been reported elsewhere (*17*). Large deaminase crystals were grown at 20 °C by the hanging drop vapor diffusion method under conditions similar to those reported previously (*20*). Briefly, 2 μL of ACC deaminase (15 mg/mL) were mixed with an equal volume of the reservoir solution containing 0.1 M Hepes (pH 7.5), 20−22.5% PEG 4000, and 10% 2-propanol and equilibrated against the reservoir solution. The cocrystals of ACC deaminase with various ligands were obtained under similar conditions using a mixture of the enzyme with 5 mM concentrations of the respective ligands (ACC, α-ketobutyrate, ACP, and two D-amino acids, D-vinylglycine and β-chloro-D-alanine). Before data collection, all crystals were transferred stepwise to a cryoprotection solution containing all components of the reservoir solution and 20% ethylene glycol, flash cooled, and stored in liquid propane. A complete data set for each crystal was collected at 100 °K on an ADSC Quantum 315 CCD area detector (Poway, CA) at the beamline X12B at the National Synchrotron Light Source, Brookhaven National Laboratory (Upton, NY). The native and complex crystals of ACC deaminase diffract to resolutions ranging from 2.5 to 2.0 Å. The diffraction images were integrated and scaled using the HKL2000 package (*21*). All crystals are isomorphous and belong to space group $P2_12_12_1$ with unit cell dimensions $a = 67.7$ Å, $b = 68.7$ Å, $c = 351.6$ Å, and contain four ACC deaminase monomers per asymmetric unit. The calculated Matthews coefficient V_m is 2.79 Å^3 Da^{-1}, corresponding to 55.9% (v/v) solvent content. The data collection statistics for all crystals are listed in Table 1.

Structure Determination and Refinement. The crystal structure of native ACC deaminase was solved by the molecular replacement method with the program MOLREP (*22*) using the coordinates of yeast ACC deaminase (PDB code 1F2D) (*23*) as a search model. The *Pseudomonas* and yeast ACC deaminases share about 60% sequence identity. The initial model was limited to polyalanines in order to minimize any model bias. The positions of all four monomers in the asymmetric unit were found by MOLREP. The subsequent refinements were carried out using the CNS program (*24*). Manual inspection and model building was done using the program O (*25*). All side chains were built in the model during the course of the refinement. The density for the bound PLP was clearly visible from the initial map and was included in the model early in the refinement. Several rounds of refinement including positional, simulated annealing, and individual *B*-factor refinements were carried out, which resulted in an *R*-factor and R_{free} of 26.0% and 30.0%, respectively. Water molecules were then identified using the water_pick routine of CNS and included in the model, provided that they satisfied good hydrogen bond geometry with the enzyme groups. The final model consists of four ACC deaminase peptide chains, 4 PLP molecules, 4 sulfate molecules, and 325 water molecules. The regions

Table 1: Data Collection and Refinement Statistics for ACCD Complexes

	native	ACC	ACP	β-Cl-D-Ala	D-VG	α-KB
Data Collection						
wavelength (Å)	1.1000	1.1000	1.1000	0.97830	0.97780	0.97904
resolution (Å)	40.0−2.0	50.0−2.1	50.0−2.5	30.0−2.10	30.0−1.97	30.0−1.99
outer shell (Å)	2.07−2.00	2.18−2.10	2.59−2.50	2.18−2.10	2.04−1.97	2.06−1.99
total reflns	672258	638899	239817	631733	1468100	769447
unique reflns	98751	95603	54030	96447	115351	112131
R_{sym}[a]	0.056 (0.291)[b]	0.060 (0.472)	0.078 (0.310)	0.123 (0.512)	0.052 (0.360)	0.077 (0.520)
completeness (%)	87.5 (49.2)	98.1 (85.2)	93.4 (96.8)	99.0 (100.0)	99.6 (99.0)	99.1 (91.8)
redundancy	6.8 (5.1)	6.7 (4.2)	4.4 (4.3)	6.6 (6.8)	12.7 (10.6)	6.9 (4.2)
av ($I/\sigma(I)$)	29.4 (4.8)	21.8 (2.8)	15.9 (4.0)	14.8 (2.9)	44.5 (9.2)	18.5 (2.1)
Refinement Statistics						
resolution (Å)	40.0−2.00	50.0−2.10	50.0−2.50	30.0−2.10	30.0−1.97	30.0−2.00
no. of reflns in working set	91889	86613	50342	91526	109483	104920
no. of reflns in test set	4851	4570	2689	4833	5765	5550
R_{cryst}[c]	0.215	0.215	0.202	0.227	0.214	0.219
R_{free}[d]	0.250	0.252	0.248	0.267	0.250	0.254
no. of non-hydrogen protein atoms	10083	10072	10072	10068	10083	10062
no. of solvent atoms	325	581	361	410	410	516
no. of ligand atoms	80	88	92	84	84	84
av B (Å^2)						
for protein atoms	36.4	36.1	37.7	42.4	41.9	37.9
for ligand atoms	48.2	32.1	32.0	44.1	39.8	47.4
RMS deviation						
bond length (Å)	0.010	0.010	0.009	0.011	0.010	0.010
bond angle (deg)	1.56	1.55	1.48	1.59	1.56	1.57

[a] $R_{sym} = \sum|(I - \langle I\rangle)|/\sum(I)$, where I is the observed integrated intensity, $\langle I\rangle$ is the average integrated intensity obtained from multiple measurements, and the summation is over all observed reflections. [b] Values in the parentheses represent those for the outer resolution shell. [c] $R_{cryst} = \sum||F_{obs}| - k|F_{calc}||/\sum|F_{obs}|$, where F_{obs} and F_{calc} are the observed and calculated structure factors, respectively. [d] R_{free} is calculated as R_{cryst} using 5% of the reflection data chosen randomly and omitted from the refinement.

from residues 129 through 140 in monomers A, B, and D have no visible electron densities and are considered disordered. For the structures of enzyme−ligand complexes, the refinements were carried out starting from the native ACC deaminase structure. The various ligand molecules were included in the model when difference electron densities warranted the unambiguous positioning of the ligands. The structure models, the topology, and the parameter files of these ligands were generated with the PRODRG server (*26*). The refinement statistics for each complex are given in Table 1.

Site-Directed Mutagenesis and Enzyme Purification. The *Sac-Nde*I fragment from pQNt23, which codes for the wild-type ACC deaminase, was cloned into pET28b(+) (Stratagene, La Jolla, CA). Using the gene insert in pET28b(+) as the template, all of the site specific mutations were introduced by using the QuickChange site-directed mutagenesis kit (Amersham, Arlington Heights, IL). The following primers were used to introduce the point mutations where the sequence in bold denotes the codon change for the mutation: Y268F forward, 5′-CGCGGGT-CCGGAA**TTC**-GGATTGCCGAACG-3′; Y268F reverse, 5′-CGTTCGGC-AATCC**GAA**TTCC-GGACCCGCG-3′; Y294F forward, 5′-GACCGATCCCGTC**TTC**GAAGGCAAATCGATGC-3′; Y294F reverse, 5′-GCATCGATTTGCCTTC**GAA**GAC-GGGATCGGTC-3′. The mutation sites were confirmed by DNA sequencing using T7 primers and terminators (Stratagene). Each of the recombinant plasmids was used to transform *E. coli* BL21 (DE3) to overexpress the encoded mutant protein. The mutant proteins were purified by the same procedure used for the wild-type protein (*17*).

Determination of the Kinetic Parameters of ACC Deaminase. A typical 0.1 mL assay, performed in 100 mM potassium phosphate buffer (pH 8.0) at 25 °C, contained 0.9 unit of L-lactate dehydrogenase, 0.3 mM NADH, and an appropriate amount of ACC deaminase, while the ACC concentration was varied from 0.5 to 10.0 mM. The reaction was initiated by the addition of the enzyme, and the decrease in absorption of NADH was monitored at 340 nm (ϵ_m = 6220 M^{-1} cm^{-1}). A sample without the substrate was used as a control. The experimental data were fit to the Michealis−Menten equation to determine the K_m and k_{cat} values. The same assay was also used to compare the specific activities of the wild-type and the mutant proteins using 5 mM D-vinylglycine (**10**) as the substrate.

Detection of Product Formation by NMR Analysis. ACC (**1**) or D-vinylglycine (**10**) (17 mM each) was incubated at 30 °C for 24 h with an appropriate amount of ACC deaminase (0.7 mg/mL for the wild-type enzyme and 4−10 mg/mL for the mutant enzyme) in 100 mM potassium phosphate buffer prepared in D_2O (pD 8.0). The reaction mixture was then subjected to NMR analysis (Varian 500 MHz) to detect product formation.

*Synthesis of D-Vinylglycine (**10**).* This synthesis was based on a literature procedure (*27*) for the preparation of the L-isomer of vinylglycine with minor modifications.

RESULTS

Quality of the Crystal Structures. The native and various ligand bound ACC deaminase crystals diffract to resolutions ranging from 2.5 to 2.0 Å. Because of the unusually long *c*-axis (351.6 Å) of the unit cell, data were collected at a synchrotron source in order to overcome severe overlaps between diffraction spots and to obtain complete data sets to maximum resolution. All complex structures have been refined to *R*-factors of 0.202−0.227 and R_{free} of 0.248−0.269 with good geometry (Table 1). The conformations of the four

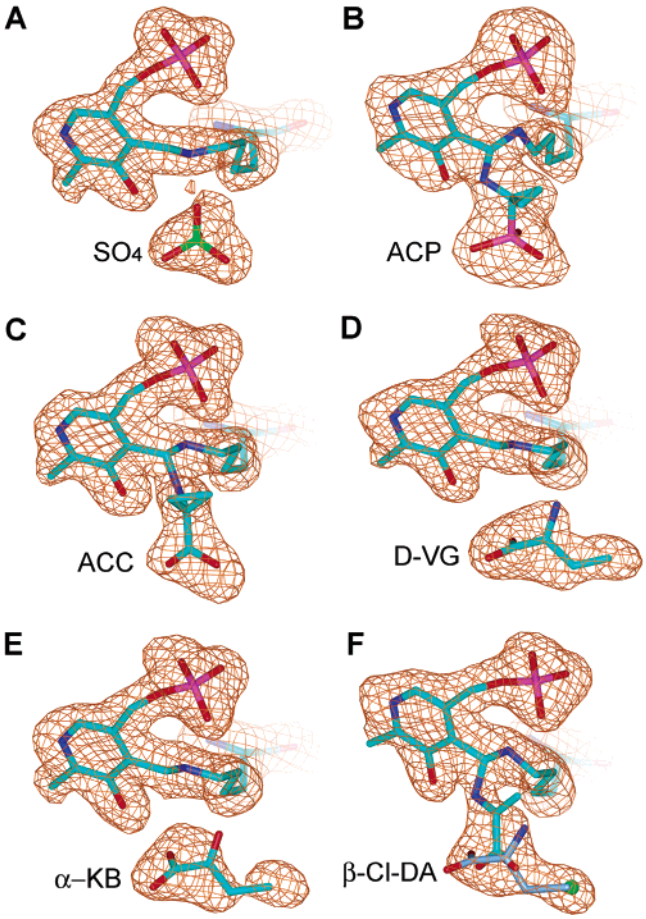

FIGURE 1: Difference $F_o - F_c$ electron density maps for the active site of *Pseudomonas* ACC deaminase complexes. (A) native enzyme; (B) enzyme−ACP (**9**) complex; (C) enzyme−ACC (**1**) complex; (D) enzyme−D-vinylglycine (**10**) complex; (E) enzyme−α-ketobutyrate (**2**) complex; (F) enzyme−β-Cl-D-Ala (**11**) complex. Only the densities for PLP, Lys51, and the respective ligands are drawn. All maps are contoured at 3σ.

crystallographically independent monomers in the asymmetric unit are very similar, with pairwise root-mean-square deviations (rmsd) of the C_α positions ranging from 0.23 to 0.36 Å. In all the structures, the continuous densities between PLP and the side chain of Lys51 are indicative of the internal aldimine. The electron densities for ACC (**1**), ACP (**9**), D-vinylglycine (**10**), and β-Cl-D-Ala (**11**) in each structure are of good quality and allowed unambiguous positioning of each ligand in the active site (Figure 1). The density for α-ketobutyrate (**2**) in the enzyme−product complex is not as well defined in comparison with the other complexes. As a result, the product in the enzyme−α-KB complex has much greater *B*-factors, indicating a higher mobility or partial occupancy of the molecule. In the complex of ACC deaminase with β-Cl-D-Ala (**11**), the difference densities at the active site suggest dual conformations of the ligand. While a Michaelis complex of the enzyme with the D-amino acid appears evident, the extra bridging density between PLP and the ligand indicates that a geminal diamine intermediate may also exist in the crystal. Thus, both β-Cl-D-Ala and an amino acrylate-PLP aldimine (*12*) were modeled in this complex with partial occupancies (Figure 1F).

Structural Comparison of the Pseudomonas and Yeast ACC Deaminases. The structure of the *Pseudomonas* ACC deaminase is very similar to that of the yeast enzyme (*23*). The overall rmsd between the C_α positions of the two enzymes is only 0.96 Å (Figure 2A). Larger deviations are found in two regions: residues 104−108 (in *Pseudomonas* enzyme numbering) where a three-residue insertion occurs in the yeast enzyme; and residues 249−258 where a two-residue insertion is found in the *Pseudomonas* enzyme. Both of these regions are located on the surface of the enzyme. In addition, the loop region in the yeast enzyme structure that corresponds to the disordered loop in the *Pseudomonas* enzyme (residue 129−140) appears to be better ordered, probably due to more favorable crystal packing interactions. Like the yeast ACC deaminase, the *Pseudomonas* enzyme contains two domains with the active site located at a deep crevice between the two domains. The overall fold of both enzymes belongs to the β family or fold group II of the PLP-dependent proteins (*10*, *28*). Close relatives of ACC deaminase in this protein family include tryptophan synthase β subunit (*29*, *30*), threonine deaminase (*31*), and *O*-acetylserine sulfhydrylase (*32*).

Although there are four monomers in the asymmetric unit of the *Pseudomonas* ACC deaminase crystal, analysis of their packing indicates that this protein likely forms dimers in solution (Figure 2B). The dimer interface (between monomers A and B, or C and D) buries 1786 Å^2 surface area on each monomer (15.5% of total surface area), which is substantially larger than the total 482 Å^2 contact area between monomer A and the adjacent dimer consisting of C and D. The majority of the buried area within the dimer is hydrophobic (1089 Å^2). The dimer of *Pseudomonas* ACC deaminase superimposes well with the yeast enzyme dimer with an rmsd for the C_α positions of 0.99 Å, indicating that the *Pseudomonas* enzyme should also have a dimeric quaternary structure similar to that of the yeast enzyme.

Active Site Structure of the Native Enzyme. The two active sites of the *Pseudomonas* enzyme dimer open to opposite directions and are separated by ~23 Å. There appear to be no direct interactions between the two active sites. The detailed protein residue arrangement at the active site of the *Pseudomonas* enzyme is very similar to that of the yeast enzyme (Figure 3). The bound PLP cofactor in the *Pseudomonas* enzyme forms an internal aldimine with Lys51 through its side chain N_ϵ amino group. The N1 atom of the PLP pyridinium ring forms a hydrogen bond with the carboxylate group of Glu295 (2.6 Å), whereas the O3′ oxygen interacts with the side chain amino group of Asn79 (3.0 Å) and a water molecule (2.6 Å). The phosphate of PLP is anchored near the *N*-terminus of an α-helix formed by residues 202−213, and interacts with the main chain amide groups of Val198, Thr199, Gly200, and Thr202, and with the side chains of Lys54, Thr199, and Thr202. Several protein residues also contact PLP through van der Waals interactions. These include Leu322, Asn50, and notably, Tyr294, the latter of which stacks against the plane of the pyridinium ring. These interactions firmly position the cofactor in the enzyme active site.

As shown in Figures 1A and 3, there exists a bound sulfate molecule in the active site of the native enzyme which interacts with the main chain amides of Asn79 and Gln80 and with the side chains of Ser78 and Tyr294. A similarly bound sulfate or phosphate molecule was also found in the yeast enzyme active site at the same location (*23*) (Figure 3). Overall, the conformation of the active site is essentially

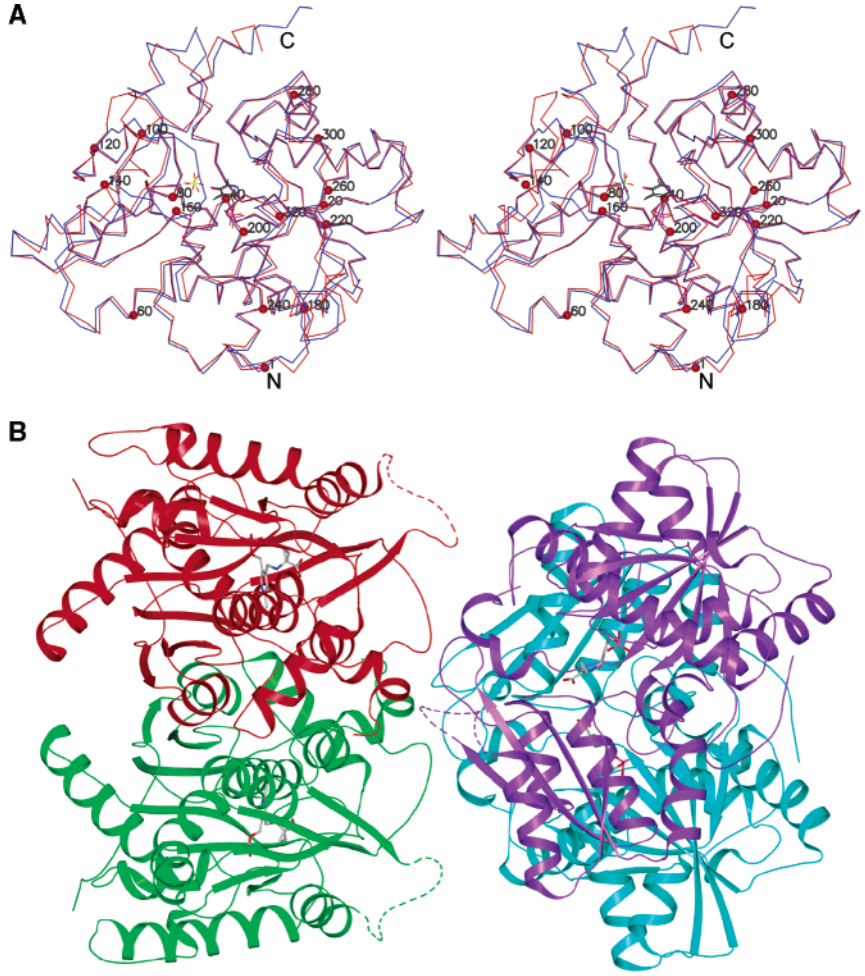

FIGURE 2: Overall structure of *Pseudomonas* ACC deaminase. (A) Stereoview of the overlaid C_α traces of the native *Pseudomonas* enzyme and the yeast enzyme monomers. The *Pseudomonas* enzyme is colored red and the yeast enzyme colored blue. Every 20th residue is labeled. The PLP cofactor and the bound sulfate are shown in stick form. (B). The packing of four crystallographic independent monomers of *Pseudomonas* ACC deaminase in the asymmetric unit. Each monomer is represented by the ribbon representation and colored differently. The bound ligand is shown in stick form.

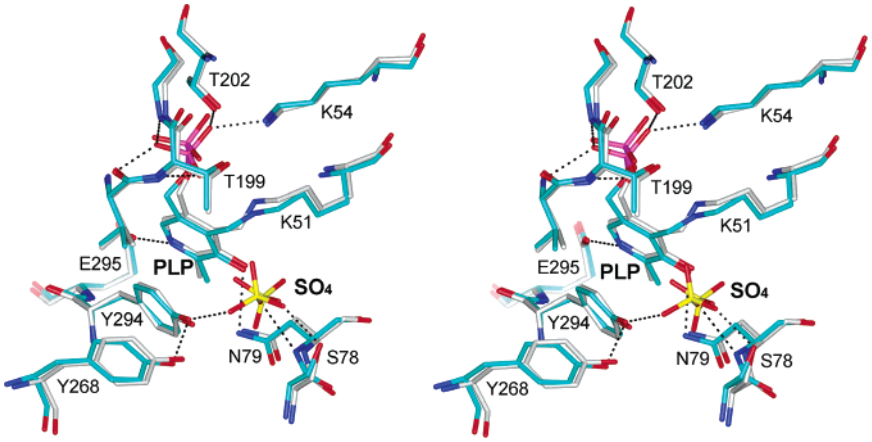

FIGURE 3: Stereoview of the overlaid active sites of the *Pseudomonas* ACC deaminase (cyan) and the yeast ACC deaminase (gray). Hydrogen bonds are indicated by dotted lines.

identical for both *Pseudomonas* and yeast enzymes (*23*), indicating that their substrate binding and catalytic mechanisms are likely the same. Therefore, mechanistic insights deduced from the structure of one enzyme should be applicable to the other.

Observation of the gem-Diamine Intermediate in the ACP and ACC Complexes. 1-Aminocyclopropane phosphonate (ACP, **9**) has been shown to be a potent inhibitor for the *Pseudomonas* enzyme with a K_i of 6.9 μM (*15*). Kinetic and UV−vis spectral analysis of the inhibited ACP−enzyme complex suggested that ACP may form a stable adduct with PLP which remains attached to the lysine anchor (Lys51) in the active site (*15*). We have recently observed directly the *gem*-diamine intermediate in the crystal structure of enzyme−ACP complex (*18*), which substantiated the earlier spectroscopic observations. It was somewhat surprising that, in the

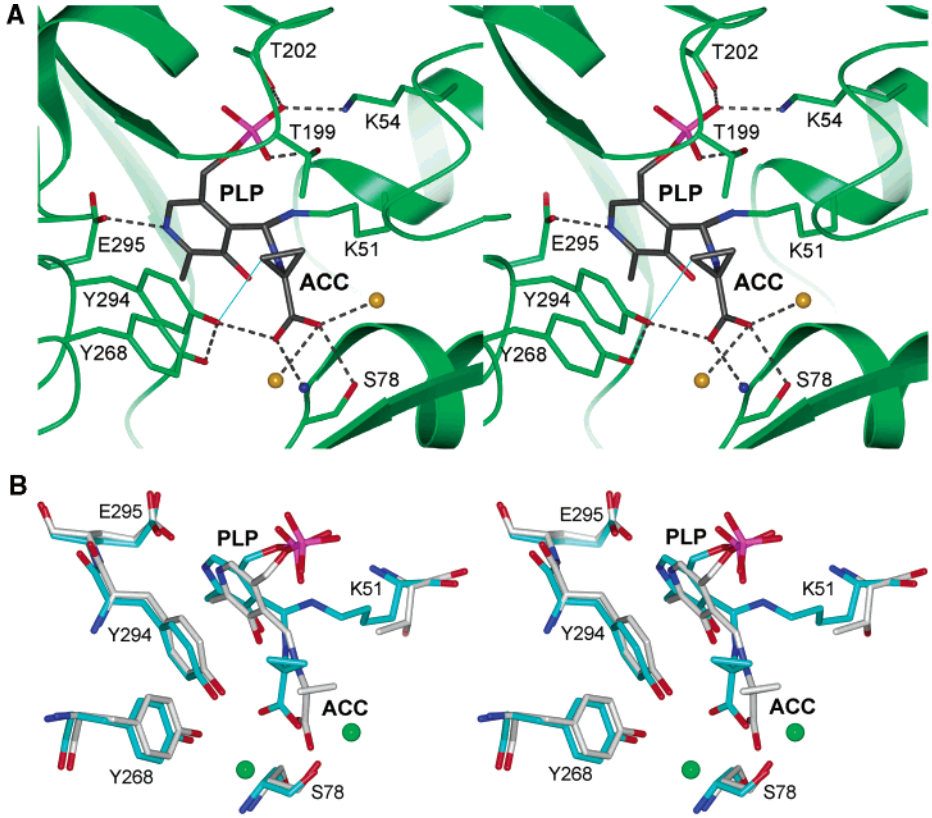

FIGURE 4: The structure of the *gem*-diamine intermediate in *Pseudomonas* ACC deaminase complexed with ACC. (A) Stereoview of the *gem*-diamine intermediate in *Pseudomonas* ACC deaminase complexed with ACC (**1**). The hydrogen bonds are indicated with dotted lines. The interaction between the Tyr294 hydroxyl group and the *pro-S* carbon of ACC is indicated by a thin blue line. (B) Stereoview of the overlaid active sites of the *Pseudomonas* ACC deaminase−ACC (**1**) complex (cyan) and the yeast K51T mutant deaminase complexed with ACC (gray). The two water molecules interacting with the bound ligand in the *Pseudomonas* enzyme are shown as small spheres.

cocrystal of ACC deaminase grown in the presence of ACC, a structure resembling the *gem*-diamine intermediate is also observed between PLP, the Lys51 side chain, and ACC (Figures 1C and 4A). It appears that the reaction stops at this *gem*-diamine step under the crystallization conditions for ACC deaminase. A similar phenomenon has previously been observed only in the crystal structure of histidinol phosphate aminotransferase where a *gem*-diamine intermediate is found in the enzyme−substrate complex (*33*). It is possible that restrictions in protein movement imposed by crystal contacts contribute to trap this supposedly transient species.

In the enzyme−ACC complex, the position of ACC is superimposable with that of ACP in the enzyme−ACP complex, and the bound ACC makes specific interactions with the enzyme similar to those observed in the enzyme−ACP structure (*18*). Here the hydroxyl group of Tyr294 is in close contact with the cyclopropane ring of ACC at the *pro-S* methylene position (3.0 Å). It also forms hydrogen bonds with the carboxylate group of ACC (2.7 Å), and with the nearby Tyr268 hydroxyl group (2.8 Å). Additionally, the carboxylate group of ACC occupies the same site as the phosphonate group of ACP in the enzyme−ACP complex structure and interacts with the main chain amide of Asn79 and the side chain hydroxyl of Ser78. In this *gem*-diamine complex, the conformation of PLP and Lys51 remains essentially the same as that observed in the internal aldimine of the native enzyme. Interestingly, when compared to the recently reported structure of yeast ACC deaminase K51T mutant complexed with ACC (*34*), the PLP−ACC external aldimine adduct (**5**) in the yeast enzyme appears to have shifted outward by about 1.5 Å relative to those in the internal aldimine and *gem*-diamine complexes of the *Pseudomonas* enzyme (Figure 4B).

Site-Directed Mutagenesis of Tyr294 and Tyr268. The fact that Tyr294 is located near the cyclopropane ring in the active site of ACC deaminase strongly suggested a direct catalytic role for this residue in the ring-opening reaction. The reactivity of Tyr294 may be enhanced by hydrogen bonding to Tyr268, which is only 2.8 Å away. These two tyrosine residues are strictly conserved among the more than twenty known ACC deaminase homologues. The conserved presence of the potential two-tyrosine relay system in ACC deaminase homologues suggests a significant function for this tyrosine pair.

To probe the possible involvement of the two tyrosine residues in the reaction, the Y294F and Y268F mutants were prepared, both of which exhibited chromatographic behavior and spectral properties identical with those of the wild-type enzyme. The PLP content in the Y268F and Y294F mutant proteins is also the same as that observed for the wild-type enzyme. These mutant proteins are capable of binding ACC in the active site as shown by the decrease of the absorption at 420 nm and the increase of the absorption at 327 nm upon incubation with ACC. However, no ACC deaminase activity of the Y294F mutant enzyme was detected using the coupled lactate dehydrogenase/NADH assay, and no keto product was generated as assessed by ^{1}H NMR spectroscopy after a 24-h incubation period with the substrate. Likewise, the activity of the Y268F mutant is also dramatically diminished. The

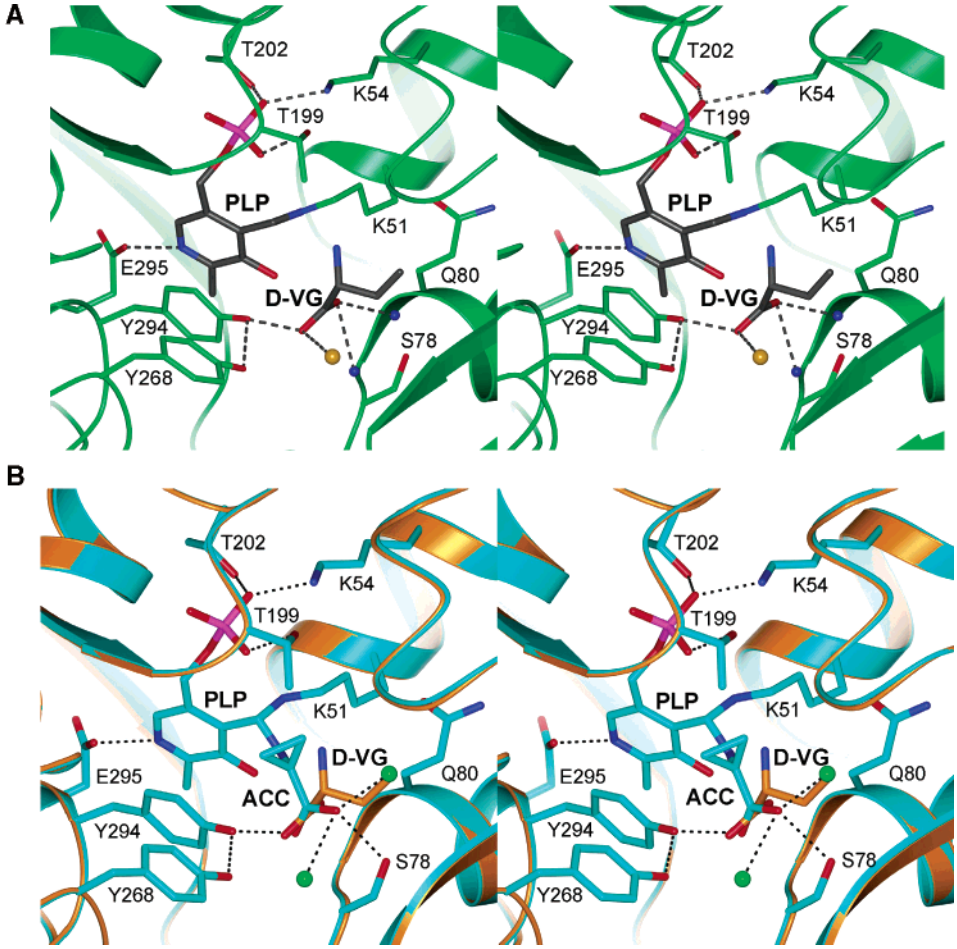

FIGURE 5: The Michaelis complex structure of the *Pseudomonas* ACC deaminase with D-vinylglycine (**10**). (A) Stereoview of D-VG bound at the enzyme active site. (B) Stereoview of the overlaid active sites of enzyme−ACC complex (cyan) and enzyme complexed with D-VG (orange). Hydrogen bonds in the enzyme−ACC complex are indicated with dotted lines. The two active-site water molecules in the enzyme−ACC complex are shown as green balls.

K_m of the Y268F protein remains unchanged (1.97 mM), but its k_{cat} (1.2 min^{-1}) is less than 2% of that of the wild-type enzyme (70 min^{-1}). Clearly, both Tyr294 and Tyr268 play critical roles in the activity of ACC deaminase.

Structure of ACC Deaminase Complexed with D-Vinylglycine. Previous mechanistic studies of ACC deaminase have shown that ACC deaminase can abstract the α-hydrogen from D-vinylglycine (D-VG, **10**) and a few other D-amino acids and catalyze the deamination of these α-amino acids at much slower rates (about 8% of the V_{max} for ACC) (*12*). The corresponding L-amino acids, on the other hand, are not substrates for this enzyme (*12*). In the crystal structure of ACC deaminase complexed with D-VG, the electron density for the D-amino acid is well defined, and is detached from PLP, consistent with the formation of a Michaelis enzyme−substrate complex (Figures 1D and 5A).

In comparison with ACC and ACP in the *gem*-diamine intermediate conformation (Figures 1C and 1B), D-VG is rotated around the carbon atom of the carboxylate group by about 60°, which moves the amino group and the α-carbon away from PLP by 2.5 and 1.7 Å, respectively (Figure 5B). The distance between the amino group of D-VG and the C-4′ position of PLP is now 3.4 Å. D-VG binds at the active site mostly through interactions between its carboxylate group and the main chain amides of Asn79, Gln80, and the hydroxyl group of Tyr294. Because of the rotation of the carboxylate group, Ser78 is no longer in contact with the carboxylate oxygen of D-VG (separated by 4 Å), but is close to its side chain C_β group (3.1 Å). In this complex, Tyr294 remains hydrogen bonded to the carboxylate group of D-VG, and is 3.7 Å away from the C_α position of D-VG.

Inspection of the D-VG−enzyme complex reveals that the enzyme active site is probably better suited to accommodate a D-amino acid rather than its L-isomer, due to steric hindrance imposed mainly by the side chains of Tyr294 and Gln80. Modeling studies show that the amino group of an L-amino acid would point toward Tyr294 and the C_α carbon would project toward the C_β methylene group of the Gln80 side chain. Such positioning would produce unfavorable close contacts of the bound L-amino acid with these residues. A more important distinction between the L- and D-amino acids, however, lies in the orientation of their α-protons: the α-H of a D-amino acid would point toward Tyr294, whereas the α-H of an L-amino acid would point toward Lys51. Since ACC deaminase is only active on D-amino acids but not the L-isomers, this structural information allows the identification of Tyr294 as the likely candidate that serves as the base to abstract the α-proton. Lys51 is largely excluded from such a role because it would be inaccessible to the α-proton of D-amino acids.

Structure of ACC Deaminase Complexed with α-Ketobutyrate. In the structure of enzyme complexed with α-

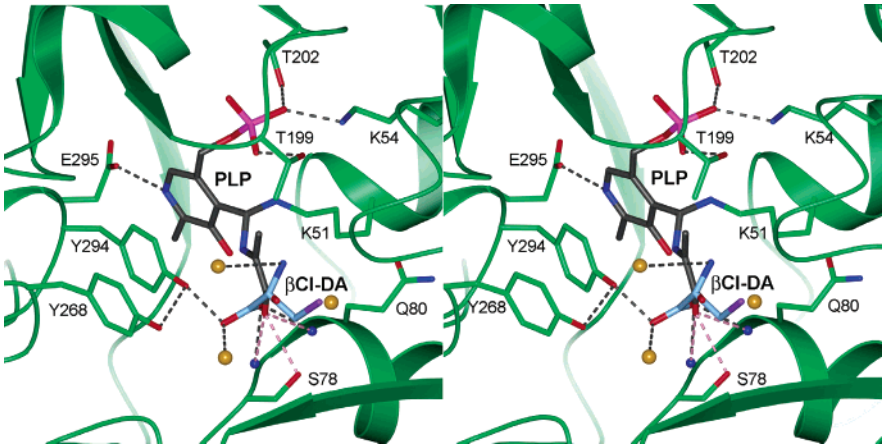

FIGURE 6: Stereoview of the active site of the *Pseudomonas* ACC deaminase in complex with β-Cl-D-Ala (**11**), showing the dual conformations of the substrate.

ketobutyrate (α-KB, **2**), the discontinuous electron density between PLP and **2** clearly shows that no external Schiff base is formed between the coenzyme and the product (Figure 1E). The density for α-KB is not as well defined as that for D-VG (**10**), and the modeled product has higher *B*-factors, indicating higher mobility of the ligand. The poor binding of the product may be due to its flexible side chain, which is freely rotatable, and its intrinsically lower binding affinity, which favors ready release of the product. The modeled product is essentially superimposable with the bound D-VG in the D-VG−enzyme complex (data not shown). It should be pointed out that binding of either D-vinylglycine or α-ketobutyrate is asymmetrical in the enzyme dimer. These two ligands are found in the active site of only one of the monomers in the dimer. The reason for this asymmetry is not clear. In contrast, both active sites of the dimer are occupied by the *gem*-diamine intermediate in the enzyme−ACP and enzyme−ACC complexes.

Structure of ACC Deaminase Complexed with β-Cl-D-Alanine. The β-substituted D-amino acids have been used as alternative substrates to probe the ability of ACC deaminase to perform β-H abstraction and γ-elimination, which are the two processes immediately following the addition of an enzyme nucleophile to the cyclopropane ring in the proposed reaction mechanism (Scheme 1, route A) (*12*). Indeed, the *Pseudomonas* ACC deaminase had been shown to be capable of converting β-substituted D-alanine to pyruvate (*12*). The crystal structure of ACC deaminase complexed with β-Cl-D-Ala (**11**) clearly shows the density for the substrate in a Michaelis complex conformation (Figure 1F). However, the additional electron density between the C-4′ position of PLP and β-Cl-D-Ala suggested that a *gem*-diamine species may also exist in the crystal structure. Thus, we modeled an amino acrylate-PLP intermediate (*12*) with partial occupancies (Figure 6). The β-Cl-D-Ala in the Michaelis complex conformation occupies essentially the same site as that of D-VG.

DISCUSSION

The series of high-resolution structures of *Pseudomonas* ACC deaminase in its native form, in complexes with ACC (**1**), ACP (**9**), α-ketobutyrate (**2**), and the alternative substrates D-VG (**10**) and β-Cl-D-Ala (**11**), provide important new mechanistic insights into the catalytic mechanism of the enzyme. The structures of the *gem*-diamine intermediates found in the ACC−enzyme and ACP−enzyme binary complexes reveal that Tyr294 is located in close proximity to the cyclopropane ring, and likely functions as the nucleophile to attack the *pro-S* carbon of ACC and initiates ring fragmentation as previously surmised (*18*). Tyrosine has been proposed to act as a nucleophile in the catalysis of several enzymes, including tyrosine kinases (*35*), trans-sialidase (*36*), and leukotriene A_4 (LTA_4) hydrolase (*37*). The reactivity of the tyrosine hydroxyl group can be enhanced by interactions with other residues in the active site. In ACC deaminase, the close interaction between Tyr294 and the ACC carboxylate group may lower the pK_a of the hydroxyl group of Tyr294, thereby increasing its nucleophilicity. In addition, Tyr294 and Tyr268 may form a charge relay system that could also enhance the reactivity of Tyr294.

The existence of such an active-site network supports the proposed nucleophilic addition mechanism (Scheme 1, route A), in which cyclopropane ring opening is initiated by the addition of the Tyr294 hydroxyl oxygen to the *pro-S* β-methylene carbon of ACC (**5** → **6**). Subsequent β-H abstraction and γ-elimination of the enzyme nucleophile (**6** → **7**) would produce the α-anion equivalent of the vinylglycyl-PLP aldimine intermediate (**7**). The most likely candidate to abstract the β-proton of **6** is Lys51 which, after release from the internal aldimine, could easily reach the β-H in **6**. As noted earlier, ACC deaminase can also perform the α-deprotonation of D-amino acids, resulting in the deamination of these substrates to their respective α-keto-acids (*12*). Analysis of the binding of D-vinylglycine (**10**) and β-Cl-D-Ala (**11**) to ACC deaminase shows that the hydroxyl group of Tyr294 is located close to the C_α atom of the D-amino acids, and thus could be in position to function as the base to abstract the α-proton of these D-amino acids.

Combined with the recent structural data on yeast ACC deaminase (*34*), multiple roles for Tyr294 (using the *Pseudomonas* enzyme numbering system) have emerged. First, its stacking interaction with the PLP pyridinium ring may help to correctly orient the cofactor in the active site. Second, Tyr294 appears to affect ACC substrate binding and may react with the α-amino group of ACC to facilitate the formation of the external aldimine between PLP and the substrate (*34*). Most significantly, the *gem*-diamine structure of the enzyme−ACC complex determined in the current

Scheme 2

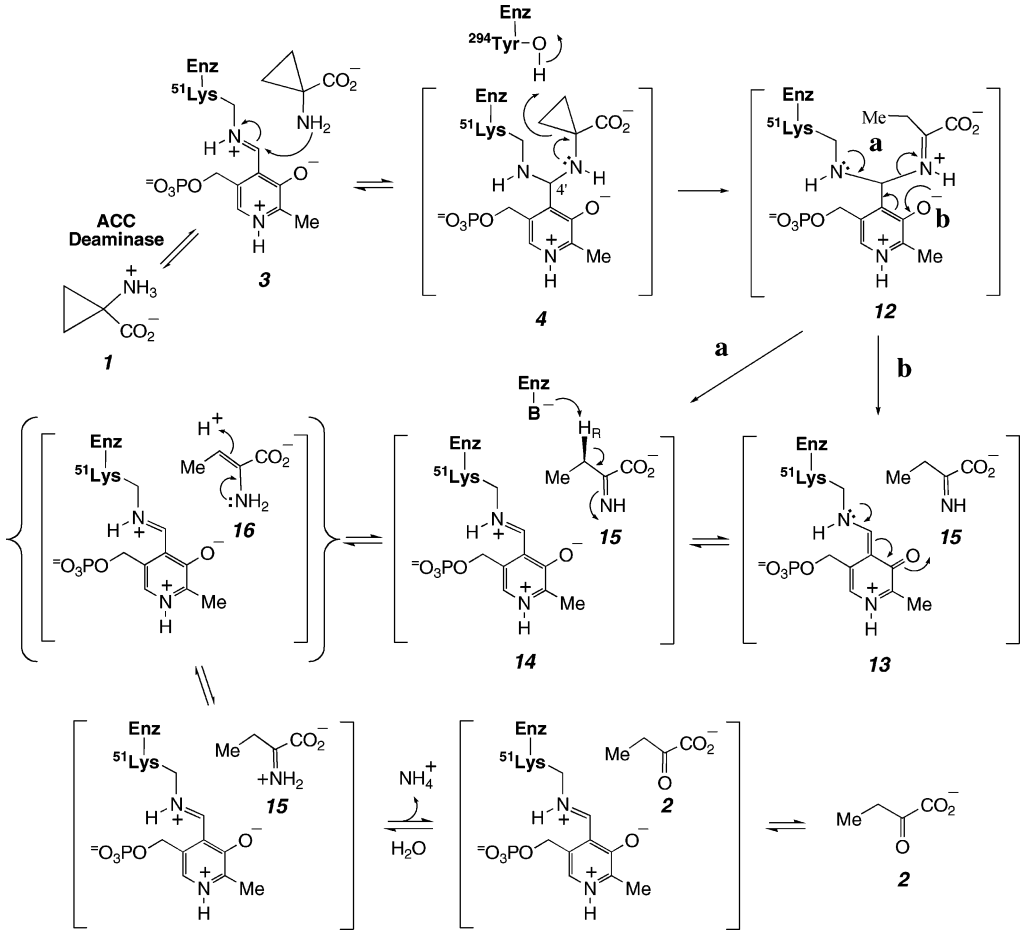

work clearly shows that the hydroxyl group of Tyr294 is within close proximity to the *pro-S* β-carbon of ACC, implicating the direct involvement of Tyr294 in the cyclopropane ring-opening reaction. Results from the mutagenesis studies by Ose et al. (*34*) and by us corroborate the essential catalytic role(s) assigned to Tyr294. Further analyses of the structures of the *Pseudomonas* enzyme complexed with D-amino acids also reveal that Tyr294 may be in position to function as a base to abstract the α-proton in the deamination of D-amino acids. The strict stereospecificity of ACC deaminase to act only on the D-amino acids but not L-amino acids is consistent with the special orientation of Tyr294 found in these structures. Notably, this particular role for Tyr294 to deprotonate the α-H of D-amino acids has also been suggested by Ose et al. (*34*).

While the accumulated evidence strongly supports the nucleophilic addition mechanism in which Tyr294 functions as the nucleophile, the surprising observation of the *gem*-diamine intermediate in both ACP and ACC complexed enzyme crystal structures may suggest an alternative mechanism in which Tyr294 serves as a general acid catalyst. In this mechanism (Scheme 2), the *gem*-diamine **4** is no longer a transient species between the internal and external aldimine stages, but a central intermediate enabling turnover to proceed. In many ways, the cyclopropane ring behaves as an alkene due to its relatively low HOMO (highest occupied molecular orbital) energy and great polarizability (*38*). This is particularly evident in its interaction with an electron deficient species, such as a proton. Hence, ring opening by protonation can be envisioned as an alternative mechanistic possibility for ACC deaminase (*39*). As depicted in Scheme 2, the ring cleavage may be facilitated by an edge- or a corner-protonation reaction promoted by Tyr294, with the assistance of the lone pair electrons on the nitrogen atoms in a "pull-and-push" mode of action (**4** → **12** → **14** + **15**, pathway a). The subsequent $C_{4'}$−N bond cleavage could also be assisted by charge delocalization through the PLP coenzyme in an overall "protonation-charge relay" pathway (**4** → **12** → **13** → **14** + **15**, pathway b). Meanwhile, Tyr268, which is accessible to the bulk solvent and interacts closely with Tyr294, may serve to transfer a proton from the surrounding solvent to the active site. A handful of examples are known where tyrosine functions as a general acid catalyst in enzyme catalysis. An established case is the reaction catalyzed by 3-oxo-Δ^5-steroid isomerase in which Tyr14 stabilizes the dienolate intermediate via either hydrogen bonding or proton transfer to the C-3 oxygen of the substrate (*40*). A similar electrophilic catalysis has also been proposed for the isomerization of the isoprene unit catalyzed by isopentenyl diphosphate (IPP):dimethylallyl diphosphate (DMAPP) isomerase. The crystal structure of the isomerase from *E. coli* reveals that Tyr104 is likely the proton source transferred, perhaps via Glu116, to the double bond of IPP during turnover (*41*).

As shown in Scheme 2, in the next step of the reaction catalyzed by ACC deaminase (**15** → **16**), a general base from the enzyme abstracts the β-proton from **15**. This step is incorporated in the mechanism to account for the solvent hydrogen exchange observed at C-3 in product **2** when the reaction is carried out in D_2O (*12*, *13*). Analysis of the

enzyme and D-VG complex structure (Figure 5) suggests that the most suitable candidate for this base is Ser78, whose side chain hydroxyl group would be about ~3 Å away from the C_β of **15**. Thus, Ser78 may have dual functions in this mechanism (Scheme 2). It may serve as an anchor in substrate binding, and it may also act as the base to abstract the β-H from **15** after ring cleavage. The fact that the S78A mutant is catalytically inactive is consistent with an important role in this mechanism (*17*). Significantly in this mechanism, the ring-opening event would bypass the formation of the external aldimine (**5**). In addition, the formation of the vinylglycyl-PLP α anion intermediate (**7**), which is a necessary step in the turnover of D-VG (**10**), is no longer part of the pathway. Although this new mechanism is drastically different from what has been proposed before and is unprecedented for PLP-dependent enzymes, it is nevertheless compatible with the chemical and structural data obtained thus far. Clearly, more experiments are needed in order to determine the exact role of Tyr294 in the ACC deaminase-catalyzed reaction.

In summary, structural analyses of the *Pseudomonas* ACC deaminase in complex with various substrates/inhibitors reveal detailed interactions between these substrates/inhibitors and protein residues at the active site of the enzyme. These studies provide a rare glimpse of the typically elusive *gem*-diamine intermediate of a PLP-dependent enzyme reaction. Most importantly, these structural data implicate Tyr294 as the key catalytic residue in ACC deaminase. It likely serves as the nucleophile in a "nucleophilic addition" mechanism for the cyclopropane ring-opening reaction. Alternatively, it may function as a general acid in a "push-and-pull" mechanism which makes advantageous use of the *gem*-diamine state. Thus, the cleavage of ACC (**1**) to α-ketobutyrate (**2**) by ACC deaminase clearly represents an intriguing conversion beyond the common scope entailed by PLP-dependent catalysts. Further studies are underway to distinguish between these two mechanisms.

REFERENCES

1. Yang, S. F., and Hoffman, N. E. (1984) Ethylene Biosynthesis and its Regulation in Higher Plants, *Annu. Rev. Plant Physiol. 35*, 155−189.
2. Adams, D. O., and Yang, S. F. (1979) Ethylene Biosynthesis: Identification of 1-aminocyclopropane-1-carboxylic Acid as an Intermediate in the Conversion of Methionine to Ethylene, *Proc. Natl. Acad. Sci. U.S.A. 76*, 170−174.
3. White, M. F., Vasquez, J., Yang, S. F., and Kirsch, J. F. (1994) Expression of apple 1-aminocyclopropane-1-carboxylate synthase in *Escherichia coli*: kinetic characterization of wild-type and active-site mutant forms, *Proc. Natl. Acad. Sci. U.S.A. 91*, 12428−12432.
4. Capitani, G., McCarthy, D. L., Gut, H., Grutter, M. G., and Kirsch, J. F. (2002) Apple 1-aminocyclopropane-1-carboxylate synthase in complex with the inhibitor L-aminoethoxyvinylglycine. Evidence for a ketimine intermediate, *J. Biol. Chem. 277*, 49735−49742.
5. Dong, J. G., Fernandez-Maculet, J. C., and Yang, S. F. (1992) Purification and characterization of 1-aminocyclopropane-1-carboxylate oxidase from apple fruit, *Proc. Natl. Acad. Sci. U.S.A. 89*, 9789−9793.
6. Honma, M., and Shimomura, T. (1978) Metabolism of 1-Aminocyclopropane-1-carboxylic Acid, *Agric. Biol. Chem. 42*, 1825−1831.
7. Minami, R., Uchiyama, K., Murakami, T., Kawai, J., Mikami, K., Yamada, T., Yokoi, D., Ito, H., Matsui, H., and Honma, M. (1998) Properties, sequence, and synthesis in *Escherichia coli* of 1-aminocyclopropane-1-carboxylate deaminase from *Hansenula saturnus*, *J. Biochem. (Tokyo) 123*, 1112−1118.
8. Klee, H. J., Hayford, M. B., Kretzmer, K. A., Barry, G. F., and Kishore, G. M. (1991) Control of ethylene synthesis by expression of a bacterial enzyme in transgenic tomato plants, *Plant Cell 3*, 1187−1193.
9. Reed, A. J., Kretzmer, K. A., Naylor, M. W., Finn, R. F., Magin, K. M., Hammond, B. G., Leimgruber, R. M., Rogers, S. G., and Fuchs, R. L. (1996) Safety Assessment of 1-Aminocyclopropane-1-carboxylic Acid Deaminase Protein Expressed in Delayed Ripening Tomatoes, *J. Agric. Food Chem. 44*, 388−394.
10. Mehta, P. K., and Christen, P. (1998) in *Advances in Enzymology and Related Areas of Molecular Biology* (Purich, D. L., Ed.) pp 129−184, John Wiley & Sons, Inc., New York.
11. Jansonius, J. N. (1998) Structure, evolution and action of vitamin B6-dependent enzymes, *Curr. Opin. Struct. Biol. 8*, 759−769.
12. Walsh, C., Pascal, R. A., Jr., Johnston, M., Raines, R., Dikshit, D., Krantz, A., and Honma, M. (1981) Mechanistic studies on the pyridoxal phosphate enzyme 1-aminocyclopropane-1-carboxylate deaminase from *Pseudomonas* sp., *Biochemistry 20*, 7509−7519.
13. Liu, H.-w., Auchus, R., and Walsh, C. T. (1984) Stereochemical Studies on the Reactions Catalyzed by the PLP-Dependent Enzyme 1-Aminocyclopropane-1-carboxylate Deaminase, *J. Am. Chem. Soc. 106*, 5335−5348.
14. Hill, R. K., Prakash, S. R., Wiesendanger, R., Angst, W., Martinoni, B., Arigoni, D., Liu, H.-w., and Walsh, C. T. (1984) Stereochemistry of the Enzymatic Ring Opening of 1-Aminocyclopropanecarboxylic Acid, *J. Am. Chem. Soc. 106*, 795−796.
15. Erion, M. D., and Walsh, C. T. (1987) 1-Aminocyclopropanephosphonate: time-dependent inactivation of 1-aminocyclopropanecarboxylate deaminase and *Bacillus stearothermophilus* alanine racemase by slow dissociation behavior, *Biochemistry 26*, 3417−3425.
16. Li, K., Du, W., Que, N. L. S., and Liu, H.-w. (1996) Mechanistic Studies of 1-Aminocyclopropane-1-carboxylate Deaminase: Unique Covalent Catalysis by Co-enzyme B_6, *J. Am. Chem. Soc. 118*, 8763−8764.
17. Zhao, Z., Chen, H., Li, K., Du, W., He, S., and Liu, H.-w. (2003) Reaction of 1-amino-2-methylenecyclopropane-1-carboxylate with 1-aminocyclopropane-1-carboxylate deaminase: analysis and mechanistic implications, *Biochemistry 42*, 2089−2103.
18. Karthikeyan, S., Zhao, Z., Kao, C., Zhou, Q., Tao, Z., Zhang, H., and Liu, H.-w. (2004) Structural Analysis of 1-Aminocyclopropane-1-carboxylate Deaminase: Observation of an Aminyl Intermediate and Identification of Tyr294 as the Active-site Nucleophile, *Angew. Chem., Int. Ed. 43*, 3425−3429.
19. Bradford, M. M. (1976) A rapid and sensitive method for the quantitation of microgram quantities of protein utilizing the principle of protein-dye binding, *Anal. Biochem. 72*, 248−254.
20. Yao, M., Tanaka, I., and Hikichi, K. (1994) Crystallization and preliminary X-ray Structure Analysis of 1-Aminocyclopropane-1-caboxylic Acid Deaminase, *J. Struct. Biol. 113*, 251−253.
21. Otwinowski, Z., and Minor, W. (1997) Processing of x-ray diffraction data collected in oscillation mode, *Methods Enzymol. 276*, 307−326.
22. Vagin, A., and Teplyakov, A. (2000) An approach to multi-copy search in molecular replacement, *Acta Crystallogr., Sect. D: Biol. Crystallogr. 56*, 1622−1624.
23. Yao, M., Ose, T., Sugimoto, H., Horiuchi, A., Nakagawa, A., Wakatsuki, S., Yokoi, D., Murakami, T., Honma, M., and Tanaka, I. (2000) Crystal structure of 1-aminocyclopropane-1-carboxylate deaminase from *Hansenula saturnus*, *J. Biol. Chem. 275*, 34557−34565.
24. Brünger, A. T., Adams, P. D., Clore, G. M., DeLano, W. L., Gros, P., Grosse-Kunstleve, R. W., Jiang, J. S., Kuszewski, J., Nilges, M., Pannu, N. S., Read, R. J., Rice, L. M., Simonson, T., and Warren, G. L. (1998) Crystallography & NMR system: A new software suite for macromolecular structure determination, *Acta Crystallogr., Sect. D: Biol. Crystallogr. 54*, 905−921.
25. Jones, T. A., Zou, J.-Y., Cowan, S. W., and Kjeldgaard, M. (1991) Improved methods for building protein models in electron density maps and the location of errors in these models, *Acta Crystallogr. A47*, 110−119.
26. van Aalten, D. M., Bywater, R., Findlay, J. B., Hendlich, M., Hooft, R. W., and Vriend, G. (1996) PRODRG, a program for generating molecular topologies and unique molecular descriptors from coordinates of small molecules, *J. Comput.-Aided Mol. Des. 10*, 255−262.

27. Meffre, P., Vo-Quang, L., Vo-Quang, Y., and Le Goffic, F. (1989) N-(Benzyloxycarbonyl)-L-vinylglycine methyl ester from L-methionine methyl ester hydrochloride, *Synth. Commun. 19*, 3457−3468.
28. Grishin, N. V., Phillips, M. A., and Goldsmith, E. J. (1995) Modeling of the spatial structure of eukaryotic ornithine decarboxylases, *Protein Sci. 4*, 1291−1304.
29. Rhee, S., Miles, E. W., and Davies, D. R. (1998) Cryocrystallography of a true substrate, indole-3-glycerol phosphate, bound to a mutant (αD60N) tryptophan synthase $\alpha_2\beta_2$ complex reveals the correct orientation of active site αGlu49, *J. Biol. Chem. 273*, 8553−8555.
30. Weyand, M., and Schlichting, I. (1999) Crystal structure of wild-type tryptophan synthase complexed with the natural substrate indole-3-glycerol phosphate, *Biochemistry 38*, 16469−16480.
31. Gallagher, D. T., Gilliland, G. L., Xiao, G., Zondlo, J., Fisher, K. E., Chinchilla, D., and Eisenstein, E. (1998) Structure and control of pyridoxal phosphate dependent allosteric threonine deaminase, *Structure 6*, 465−475.
32. Burkhard, P., Rao, G. S., Hohenester, E., Schnackerz, K. D., Cook, P. F., and Jansonius, J. N. (1998) Three-dimensional structure of O-acetylserine sulfhydrylase from *Salmonella typhimurium*, *J. Mol. Biol. 283*, 121−133.
33. Sivaraman, J., Li, Y., Larocque, R., Schrag, J. D., Cygler, M., and Matte, A. (2001) Crystal structure of histidinol phosphate aminotransferase (HisC) from *Escherichia coli*, and its covalent complex with pyridoxal-5′-phosphate and l-histidinol phosphate, *J. Mol. Biol. 311*, 761−776.
34. Ose, T., Fujino, A., Yao, M., Watanabe, N., Honma, M., and Tanaka, I. (2003) Reaction intermediate structures of 1-aminocyclopropane-1-carboxylate deaminase: insight into PLP-dependent cyclopropane ring-opening reaction, *J. Biol. Chem. 278*, 41069−41076.
35. Cole, P. A., Burn, P., Takacs, B., and Walsh, C. T. (1994) Evaluation of the catalytic mechanism of recombinant human Csk (C-terminal Src kinase) using nucleotide analogs and viscosity effects, *J. Biol. Chem. 269*, 30880−30887.
36. Watts, A. G., Damager, I., Amaya, M. L., Buschiazzo, A., Alzari, P., Frasch, A. C., and Withers, S. G. (2003) *Trypanosoma cruzi* trans-sialidase operates through a covalent sialyl−enzyme intermediate: tyrosine is the catalytic nucleophile, *J. Am. Chem. Soc. 125*, 7532−7533.
37. Mancini, J. A., Waugh, R. J., Thompson, J. A., Evans, J. F., Belley, M., Zamboni, R., and Murphy, R. C. (1998) Structural characterization of the covalent attachment of leukotriene A3 to leukotriene A4 hydrolase, *Arch. Biochem. Biophys. 354*, 117−124.
38. Wiberg, K. B. (1987) in *The Chemistry of the Cyclopropyl Group* (Rappopor, Z., Ed.) Part 1, pp 1−26, John Wiley, New York.
39. Liu, H.-w. (1998) Coenzyme B_6-dependent novel bond cleavage reactions, *Pure Appl. Chem. 70*, 9−16.
40. Wu, Z. R., Ebrahimian, S., Zawrotny, M. E., Thornburg, L. D., Perez-Alvarado, G. C., Brothers, P., Pollack, R. M., and Summers, M. F. (1997) Solution structure of 3-oxo-Δ^5-steroid isomerase, *Science 276*, 415−418.
41. Wouters, J., Oudjama, Y., Barkley, S. J., Tricot, C., Stalon, V., Droogmans, L., and Poulter, C. D. (2003) Catalytic mechanism of *Escherichia coli* isopentenyl diphosphate isomerase involves Cys-67, Glu-116, and Tyr-104 as suggested by crystal structures of complexes with transition state analogues and irreversible inhibitors, *J. Biol. Chem. 278*, 11903−11908.

BI048878G